

2020


First Ionization Energy as the Asymptotic Limit of the Average Local Electron Energy

Amer M. El-Samman

Egor Ospadov

Viktor N. Staroverov

Follow this and additional works at: <https://ir.lib.uwo.ca/chempub>

 Part of the [Chemistry Commons](#)

First Ionization Energy as the Asymptotic Limit of the Average Local Electron Energy

Amer M. El-Samman, Egor Ospadov, and Viktor N. Staroverov*

Department of Chemistry, The University of Western Ontario,

London, Ontario N6A 5B7, Canada

(Dated: October 2, 2020)

Abstract

The first vertical ionization energy of an atom or molecule is encoded in the rate of exponential decay of the exact natural orbitals. For natural orbitals represented in terms of Gaussian basis functions, this property does not hold even approximately. We show that it is nevertheless possible to deduce the first ionization energy from the long-range behavior of Gaussian-basis-set wavefunctions by evaluating the asymptotic limit of a quantity called the average local electron energy (ALEE), provided that the most diffuse functions of the basis set have suitable shape and location. The ALEE method exposes subtle qualitative differences between seemingly analogous Gaussian basis sets and complements the extended Koopmans theorem by being robust in situations where the one-electron reduced density matrix is ill-conditioned.

Corresponding Author

*E-mail: vstarove@uwo.ca

ORCID: 0000-0002-6828-3815

1. INTRODUCTION

The vertical ionization energy (IE) of a chemical species X is the internal energy change for the process $X \rightarrow X^+ + e$, where X^+ has the molecular geometry of X and both species are in their ground electronic states. Experiments measure vertical IEs as differences between the energies of the ground vibrational state of X and vibrationally excited states of X^+ ,¹ but in quantum chemistry it is customary to focus on the purely electronic contribution

$$I = E_e(X^+) - E_e(X) \quad (1)$$

where $E_e(X)$ and $E_e(X^+)$ are the ground-state electronic energies of the initial and ionized systems. In this work, IE means exclusively the first (lowest) nonadiabatic electron removal energy defined by eq 1 for the nonrelativistic, fixed-nucleus solutions of the Schrödinger equation.

The direct way to predict an IE is to compute $E_e(X)$ and $E_e(X^+)$ separately at the same level of theory. There are also many indirect approaches (reviewed in Ref. 2) that avoid a separate calculation on the cation by relating the ground-state wavefunction of X^+ to that of X ,³⁻¹⁰ or by using the electron propagator theory.¹¹ The basic premise of such techniques is made plausible by the fact that the value of I is encoded in the exact wavefunction of X alone. Specifically, it is known that the exact ground-state electron density of an atom or molecule falls off asymptotically as^{7,12-17}

$$\rho(\mathbf{r}) \sim r^\beta \exp(-2\sqrt{2I}r) \quad (r \rightarrow \infty) \quad (2)$$

where β is a system-specific positive constant. From eq 2 there follow naive recipes for extracting I from $\rho(\mathbf{r})$, e.g.,

$$\lim_{r \rightarrow \infty} \frac{\nabla^2 \rho(\mathbf{r})}{8\rho(\mathbf{r})} = \lim_{r \rightarrow \infty} \frac{\tau_W(\mathbf{r})}{\rho(\mathbf{r})} = I \quad (3)$$

where $\tau_W(\mathbf{r}) = |\nabla \rho(\mathbf{r})|^2 / 8\rho(\mathbf{r})$. The exponent $2\sqrt{2I}$ also governs the rate of exponential decay of the natural orbitals of the system,^{7,12,15} which means that not only $\rho(\mathbf{r})$ but also many other quantities imply the IE. For instance,¹⁸

$$\lim_{r \rightarrow \infty} \frac{\tau(\mathbf{r})}{\rho(\mathbf{r})} = - \lim_{r \rightarrow \infty} \frac{\tau_L(\mathbf{r})}{\rho(\mathbf{r})} = I \quad (4)$$

where $\tau(\mathbf{r}) = \frac{1}{2} [\nabla_{\mathbf{r}} \nabla_{\mathbf{r}'} \gamma(\mathbf{r}, \mathbf{r}')]_{\mathbf{r}'=\mathbf{r}}$ is the positive-definite form of the kinetic energy density expressed in terms of the one-electron reduced density matrix (1-RDM) $\gamma(\mathbf{r}, \mathbf{r}')$ and $\tau_L(\mathbf{r}) = \tau(\mathbf{r}) - \nabla^2 \rho(\mathbf{r}) / 4$.

Unfortunately, eq 3 and eq 4 are useless in practice because they do not hold even approximately when $\rho(\mathbf{r})$, $\tau(\mathbf{r})$, and $\tau_L(\mathbf{r})$ are represented in terms of Gaussian basis functions. Such functions contain factors of the form $\exp(-\alpha_i r^2)$ which cause the ratios of eq 3 and eq 4 to diverge with increasing r (see Appendix).

Koopmans' theorem¹⁹ and its extension⁷⁻¹⁰ to correlated wavefunctions are more sophisticated techniques for extracting IEs from ground-state electron distributions. These theorems work for Gaussian basis sets but have their own limitations: IE values predicted by Koopmans' theorem for Hartree–Fock (HF) wavefunctions are not sufficiently accurate, whereas the extended Koopmans theorem (EKT) runs into numerical problems when the 1-RDM has very small eigenvalues or is not positive-definite.²⁰⁻²³

The objective of this work is to demonstrate that the idea to compute the first IE as an asymptotic limit of some ground-state quantity does not have to be abandoned. The quantity we employ for this purpose is the average local electron energy (ALEE), $\bar{\epsilon}(\mathbf{r})$, defined below, which has the formal property²⁴

$$\lim_{r \rightarrow \infty} \bar{\epsilon}(\mathbf{r}) = -I \quad (5)$$

We will show that proper construction of $\bar{\epsilon}(\mathbf{r})$ in a finite basis set and subsequent analytic evaluation of the asymptotic limit do furnish the first IE. This technique may be regarded as the most direct practical way of extracting IEs from approximate wavefunctions.

2. AVERAGE LOCAL ELECTRON ENERGY

The main ingredient of the ALEE and EKT is the generalized Fock operator,²⁵⁻²⁷ also known as the extended HF operator,^{28,29} Koopmans operator,³⁰ Lagrangian matrix,³¹ and by other names. This operator is defined by its integral kernel, which for spin-compensated systems may be written in the spin-free form as

$$G(\mathbf{r}, \mathbf{r}') = \hat{h}(\mathbf{r})\gamma(\mathbf{r}, \mathbf{r}') + 2 \int \frac{\Gamma(\mathbf{r}, \mathbf{r}_2; \mathbf{r}', \mathbf{r}_2)}{|\mathbf{r} - \mathbf{r}_2|} d\mathbf{r}_2 \quad (6)$$

where

$$\hat{h}(\mathbf{r}) = -\frac{1}{2}\nabla^2 + v(\mathbf{r}) \quad (7)$$

is the one-electron core Hamiltonian, $\gamma(\mathbf{r}, \mathbf{r}')$ is the 1-RDM, and $\Gamma(\mathbf{r}_1, \mathbf{r}_2; \mathbf{r}'_1, \mathbf{r}'_2)$ is the 2-RDM.

Application of the EKT consists of solving the eigenvalue problem⁹

$$\int G(\mathbf{r}, \mathbf{r}')\psi_k(\mathbf{r}') d\mathbf{r}' = (-I_k) \int \gamma(\mathbf{r}, \mathbf{r}')\psi_k(\mathbf{r}') d\mathbf{r}' \quad (8)$$

where I_k are electron removal energies and $\psi_k(\mathbf{r}')$ are the associated amplitudes. In practice, eq 8 is solved in matrix form¹⁰

$$\mathbf{G}\mathbf{d}_k = (-I)_k\mathbf{P}\mathbf{d}_k \quad (9)$$

where \mathbf{G} , \mathbf{P} , and \mathbf{d}_k are matrix representations of $G(\mathbf{r}, \mathbf{r}')$, $\gamma(\mathbf{r}, \mathbf{r}')$, and $\psi_k(\mathbf{r})$, respectively.

The ALEE function is defined as²⁴

$$\bar{\epsilon}(\mathbf{r}) = \frac{G(\mathbf{r}, \mathbf{r})}{\rho(\mathbf{r})} \quad (10)$$

where $\rho(\mathbf{r}) \equiv \gamma(\mathbf{r}, \mathbf{r})$. The quantity $G(\mathbf{r}, \mathbf{r})$ may be expressed in different ways^{24,32-35} that are equivalent in a complete basis set but not in a finite one. One such expression is obtained by substituting eq 6 into eq 10:

$$\bar{\epsilon}(\mathbf{r}) = \frac{\tau_L(\mathbf{r})}{\rho(\mathbf{r})} + v(\mathbf{r}) + v_{ee}(\mathbf{r}) \quad (11)$$

where

$$\tau_L(\mathbf{r}) = -\frac{1}{2} [\nabla^2 \gamma(\mathbf{r}, \mathbf{r}')]_{\mathbf{r}'=\mathbf{r}} \quad (12)$$

and

$$v_{ee}(\mathbf{r}) = \frac{2}{\rho(\mathbf{r})} \int \frac{\Gamma(\mathbf{r}, \mathbf{r}_2; \mathbf{r}, \mathbf{r}_2)}{|\mathbf{r} - \mathbf{r}_2|} d\mathbf{r}_2 \quad (13)$$

is the effective electron-electron interaction potential. The name ALEE owes to the fact that eq 11 may be interpreted as the sum of local kinetic and potential energies per electron.

For calculations using finite basis sets, it is crucial^{34,35} to employ not eq 6 but the spectral representation of $G(\mathbf{r}, \mathbf{r}')$ which restricts the domain of this kernel to the appropriate vector subspace. This representation is

$$G(\mathbf{r}, \mathbf{r}') = 2 \sum_{k=1}^K \lambda_k g_k(\mathbf{r}) g_k^*(\mathbf{r}') \quad (14)$$

where $g_k(\mathbf{r})$ are basis-set expansions of the eigenvectors of \mathbf{G} , λ_k are the associated eigenvalues, and K is the dimension of the space spanned by the spatial orbitals from which the wavefunction, RDMs, and $G(\mathbf{r}, \mathbf{r}')$ are built. The factor of 2 arises from spin summation. Substitution of eq 14 into eq 10 gives²⁴

$$\bar{\epsilon}(\mathbf{r}) = \frac{2}{\rho(\mathbf{r})} \sum_{k=1}^K \lambda_k |g_k(\mathbf{r})|^2 \quad (15)$$

which is how we compute the ALEE here. Within a finite Gaussian basis set, the output of eq 15 retains the correct shape and smoothness of the exact (basis-set-limit) ALEE,^{34,35}

whereas the output of formulas such as eq 11 is characterized by wild oscillations and divergences.^{36,37}

The spectral representation of the 1-RDM is

$$\gamma(\mathbf{r}, \mathbf{r}') = 2 \sum_{k=1}^K n_k \chi_k(\mathbf{r}) \chi_k^*(\mathbf{r}') \quad (16)$$

where $\chi_k(\mathbf{r})$ are natural orbitals and n_k are their occupation numbers ($0 \leq n_k \leq 1$).

For a closed-shell N -electron Slater determinant of spatial canonical orbitals $\phi_k(\mathbf{r})$ with eigenvalues ϵ_k , we have $K = N/2$, $g_k(\mathbf{r}) = \phi_k(\mathbf{r})$ and $\lambda_k = n_k \epsilon_k$, where $n_k = 1$ for occupied orbitals and 0 for unoccupied, so eq 15 may be written as

$$\bar{\epsilon}(\mathbf{r}) = \frac{2}{\rho(\mathbf{r})} \sum_{i=1}^{N/2} \epsilon_i |\phi_i(\mathbf{r})|^2 \quad (17)$$

with $\rho(\mathbf{r}) = \sum_{i=1}^{N/2} |\phi_i(\mathbf{r})|^2$. For a complete active space (CAS) self-consistent-field (SCF) wavefunction, K is the total number of core and active-space orbitals. In the full configuration interaction (FCI) method, K is the dimension of the space spanned by the one-electron basis set (for M linearly independent basis functions, $K = M$). An ALEE is never more difficult to calculate than the underlying wavefunction.

3. ASYMPTOTIC LIMIT OF THE ALEE

According to eq 11, the $r \rightarrow \infty$ limit of $\bar{\epsilon}(\mathbf{r})$ should be the same as that of the ratio $\tau_L(\mathbf{r})/\rho(\mathbf{r})$ because the terms $v(\mathbf{r})$ and $v_{ee}(\mathbf{r})$ vanish at infinity. For exact wavefunctions, the asymptotic limit of $\tau_L(\mathbf{r})/\rho(\mathbf{r})$ is given by eq 4, whence eq 5 is obtained. Within a Gaussian basis set, however, the ratio $\tau_L(\mathbf{r})/\rho(\mathbf{r})$ diverges at infinity³⁶ (see Appendix) and so does the right-hand side of eq 11. We will now demonstrate that the quantity $\bar{\epsilon}(\mathbf{r})$ constructed using eq 15 always has a well-defined $r \rightarrow \infty$ limit within a basis set of Gaussian functions despite their physically incorrect fall-off rate. Moreover, under certain mild constraints on the basis set, this limit is close to the exact first IE. The essence of the ALEE method for extracting the first IE from a wavefunction is represented graphically in Fig. 1.

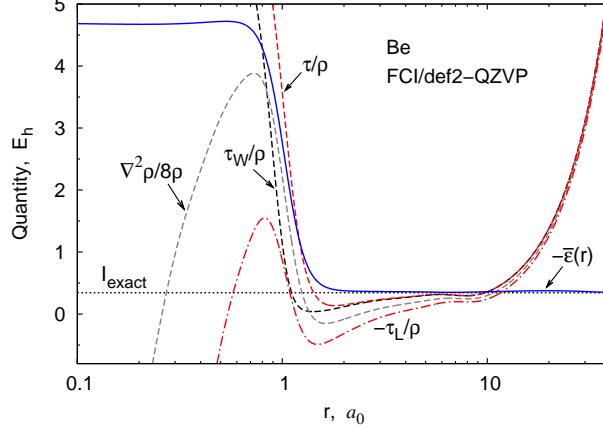


Figure 1: Various quantities computed from the FCI/def2-QZVP wavefunction of the Be atom. All of these are supposed to approach the first IE ($I_{\text{exact}} = 0.3426 E_h$) in the $r \rightarrow \infty$ limit, but only $-\bar{\epsilon}(\mathbf{r})$ does so (approximately). The small deviations $-\bar{\epsilon}(\mathbf{r})$ from the expected behavior at large r are basis-set effects explained in ref 38.

3.1. General procedure

The theoretical foundation for the proposed method is eq 5 with $\bar{\epsilon}(\mathbf{r})$ given by eq 15. To evaluate the $r \rightarrow \infty$ limit of this $\bar{\epsilon}(\mathbf{r})$, we need to rewrite eq 15 explicitly in terms of one-electron basis functions. Suppose we have a basis set of M real functions $f_\mu(\mathbf{r})$ ($\mu = 1, 2, \dots, M$). Then the eigenfunctions of the generalized Fock operator are given by

$$g_k(\mathbf{r}) = \sum_{\mu=1}^M b_{\mu k} f_\mu(\mathbf{r}) \quad (18)$$

where the coefficients $b_{\mu i}$ are determined by diagonalizing the matrix \mathbf{G} after transforming it to an auxiliary orthonormal basis set. Substitution of eq 18 into eq 14 gives

$$G(\mathbf{r}, \mathbf{r}') = 2 \sum_{\mu=1}^M \sum_{\nu=1}^M G_{\mu\nu} f_\mu(\mathbf{r}) f_\nu(\mathbf{r}') \quad (19)$$

where

$$G_{\mu\nu} = \sum_{k=1}^K \lambda_k b_{\mu k} b_{\nu k} \quad (20)$$

The natural orbital expansions are

$$\chi_k(\mathbf{r}) = \sum_{\mu=1}^M c_{\mu k} f_\mu(\mathbf{r}) \quad (21)$$

where the coefficients $c_{\mu i}$ are obtained by a similar diagonalization of the density matrix \mathbf{P} . Substitution of eq 21 into eq 16 gives

$$\gamma(\mathbf{r}, \mathbf{r}') = 2 \sum_{\mu=1}^M \sum_{\nu=1}^M P_{\mu\nu} f_{\mu}(\mathbf{r}) f_{\nu}(\mathbf{r}') \quad (22)$$

where

$$P_{\mu\nu} = \sum_{k=1}^K n_k c_{\mu k} c_{\nu k} \quad (23)$$

Using the diagonal parts of eq 19 and eq 22 in eq 10 we obtain

$$\bar{\epsilon}(\mathbf{r}) = \frac{\sum_{\mu=1}^M \sum_{\nu=1}^M G_{\mu\nu} f_{\mu}(\mathbf{r}) f_{\nu}(\mathbf{r})}{\sum_{\mu=1}^M \sum_{\nu=1}^M P_{\mu\nu} f_{\mu}(\mathbf{r}) f_{\nu}(\mathbf{r})} \quad (24)$$

Generally, $\bar{\epsilon}(\mathbf{r})$ approaches different asymptotic limits in different directions. Let us denote the asymptotic limit of $\bar{\epsilon}(\mathbf{r})$ in the direction defined by a unit vector \mathbf{u} by

$$a(\mathbf{u}) = \lim_{r \rightarrow \infty} \bar{\epsilon}(r\mathbf{u}) \quad (25)$$

and the largest (least negative) of these limits by

$$a_{\max} = \max_{\mathbf{u}} a(\mathbf{u}) \quad (26)$$

As we will see below, the IE encoded in the ALEE is

$$I_{\text{ALEE}} = -a_{\max} \quad (27)$$

Extraction of the IE from an ALEE amounts to finding the greatest (least negative) $r \rightarrow \infty$ limit of eq 24.

In principle, one can determine a_{\max} graphically by plotting the right-hand side of eq 24 in various directions, but this method is obviously inefficient. A better approach is to compute a_{\max} analytically using the fact that the asymptotic behavior of eq 24 is governed by the slowest-decaying (most diffuse) functions of the basis set and their coefficients $G_{\mu\nu}$ and $P_{\mu\nu}$. The slowest-decaying primitive functions are those that have the smallest exponent (α_0) and the highest angular quantum number l among the functions with α_0 . The rate of decay of a contracted basis function is determined by the diffuse primitive function of the contraction.

To determine a_{\max} for a given system and basis set, one needs to take into account the type, number, positions, and nodes of the slowest-decaying basis functions, as well as the angular dependence of $a(\mathbf{u})$. The problem is non-trivial in general, but has very simple solutions for many special cases. We will present four such cases which cover sufficiently many situations to demonstrate that the proposed method works.

3.2. Special cases

For notational convenience we assume that the basis functions have been ordered by the rate of their asymptotic decay, so that the slowest-decaying function is $f_1(\mathbf{r})$.

Case 1: The slowest-decaying function is a single s -type ($l = 0$) orbital, $f_1(\mathbf{r})$, centered at the origin of the coordinate axes. Using eq 24 we immediately obtain

$$a_{1s} = \lim_{r \rightarrow \infty} \bar{\epsilon}(\mathbf{r}) = \frac{G_{11}}{P_{11}} = \frac{\sum_{k=1}^K \lambda_k |b_{k1}|^2}{\sum_{k=1}^K n_k |c_{k1}|^2} \quad (28)$$

where a_{k1} and c_{k1} are the coefficients of $f_1(\mathbf{r})$ in eq 18 and eq 21, respectively. Since $f_1(\mathbf{r})$ is spherically symmetric, this limit is the same in every direction, so we take

$$a_{\max} = a_{1s} \quad (29)$$

Case 2: The slowest-decaying functions are three p -type ($l = 1$) orbitals, ($f_1 = p_x$, $f_2 = p_y$, $f_3 = p_z$) centered at the origin of the coordinate axes, and the system is oriented in such a way that each eigenfunction $g_k(\mathbf{r})$ and each natural orbital $\chi_k(\mathbf{r})$ have nonzero contributions from at most one of these functions. If these conditions are met, the asymptotic limit of $\bar{\epsilon}(\mathbf{r})$ along the x axis is determined by the contributions of $f_1(\mathbf{r})$ alone (as if it were Case 1), so

$$a_{1p}^x = \lim_{x \rightarrow \pm\infty} \bar{\epsilon}(x, y, z) = \frac{G_{11}}{P_{11}} \quad (30)$$

By a similar argument,

$$a_{1p}^y = \lim_{y \rightarrow \pm\infty} \bar{\epsilon}(x, y, z) = \frac{G_{22}}{P_{22}} \quad (31)$$

$$a_{1p}^z = \lim_{z \rightarrow \pm\infty} \bar{\epsilon}(x, y, z) = \frac{G_{33}}{P_{33}} \quad (32)$$

In general, $a_{1p}^x \neq a_{1p}^y \neq a_{1p}^z$. Owing to the special orientation of the coordinate axes, $a(\mathbf{u})$ interpolates between these three values but does not exceed the greatest of them. Therefore,

$$a_{\max} = \max\{a_{1p}^x, a_{1p}^y, a_{1p}^z\} \quad (33)$$

Note that if the p_x , p_y , and p_z functions belong to a three-dimensional irreducible representation of the point group of the system (e.g., Ne atom, CH₄ molecule), then $a(\mathbf{u})$ is isotropic: $a_{1p}^x = a_{1p}^y = a_{1p}^z$. If the system has at most cylindrical symmetry with respect to the z axis (e.g., LiF molecule), then $a_{1p}^x = a_{1p}^y \neq a_{1p}^z$, and so on.

Case 3: The slowest-decaying functions are two identical s -type Gaussians, $f_1(\mathbf{r})$ and $f_2(\mathbf{r})$, whose centers are R a.u. apart. Without loss of generality, we can assume that the coordinates of the centers are $(0, 0, \pm R/2)$. Now eq 24 gives different limits for different directions: along the z axis we get

$$a_{2s}^z = \lim_{z \rightarrow \pm\infty} \bar{\epsilon}(x, y, z) = \frac{G_{11}}{P_{11}} = \frac{G_{22}}{P_{22}} \quad (34)$$

whereas in the xy plane intersecting the z axis at $z = t$

$$\begin{aligned} a_{2s}^{xy}(t) &= \lim_{x \rightarrow \pm\infty} \bar{\epsilon}(x, y, t) = \lim_{y \rightarrow \pm\infty} \bar{\epsilon}(x, y, t) \\ &= \frac{(1 + e^{4\alpha_0 Rt})G_{11} + 2e^{2\alpha_0 Rt}G_{12}}{(1 + e^{4\alpha_0 Rt})P_{11} + 2e^{2\alpha_0 Rt}P_{12}} \end{aligned} \quad (35)$$

where $G_{11} = G_{22}$ and $P_{11} = P_{22}$ by symmetry of the system and $G_{12} = G_{21}$ and $P_{12} = P_{21}$ by symmetry of the matrices. The function $a_{2s}^{xy}(t)$ becomes stationary at $t = 0$ and $t = \pm\infty$, where it assumes the values

$$a_{2s}^{xy}(0) = \frac{G_{11} + G_{12}}{P_{11} + P_{12}} \quad (36)$$

and $a_{2s}^{xy}(\infty) = a_{2s}^z$. Analysis of the function $a_{2s}^{xy}(t)$ shows that, whenever $a_{2s}^{xy}(0)$ is a maximum, $a_{2s}^{xy}(\infty)$ is a minimum, and vice versa, depending on the values of the matrix elements. Therefore,

$$a_{\max} = \max\{a_{2s}^{xy}(0), a_{2s}^z\} \quad (37)$$

Case 4: The slowest-decaying functions are two sets of Gaussian p -type orbitals centered at the points $A = (0, 0, R/2)$ and $B = (0, 0, -R/2)$. Let us label these functions $f_1 = p_x^A$, $f_2 = p_y^A$, $f_3 = p_z^A$, $f_4 = p_x^B$, $f_5 = p_y^B$, $f_6 = p_z^B$. Assuming that the centers A and B are equivalent by symmetry, we have $G_{11} = G_{44}$, $G_{22} = G_{55}$, $G_{33} = G_{66}$, $P_{11} = P_{44}$, etc. Evaluation of the asymptotic limit of eq 24 in directions parallel to the z axis gives

$$a_{2p}^z = \lim_{z \rightarrow \pm\infty} \bar{\epsilon}(x, y, z) = \frac{G_{33}}{P_{33}} = \frac{G_{66}}{P_{66}} \quad (38)$$

For lines parallel to the x axis at $z = t$ we obtain

$$a_{2p}^x(t) = \lim_{x \rightarrow \pm\infty} \bar{\epsilon}(x, y, t) = \frac{(1 + e^{4\alpha_0 Rt})G_{11} + 2e^{2\alpha_0 Rt}G_{14}}{(1 + e^{4\alpha_0 Rt})P_{11} + 2e^{2\alpha_0 Rt}P_{14}} \quad (39)$$

which has the same analytic form as $a_{2s}^x(t)$. As shown in Fig. 2, the maximum value of $a_{2p}^x(t)$ is either

$$a_{2p}^x(0) = \frac{G_{11} + G_{14}}{P_{11} + P_{14}} \quad (40)$$

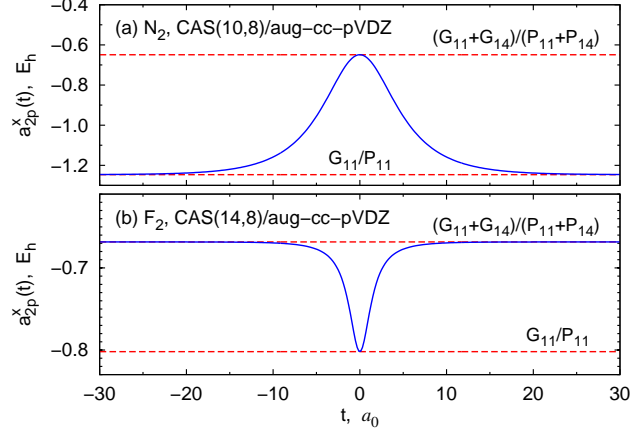


Figure 2: Directional dependence of the asymptotic limits of full-valence CASSCF ALEEs calculated using Gaussian basis sets in which the most diffuse functions are two (p_x, p_y, p_z) sets equivalent by symmetry. See Case 4 for details.

or

$$a_{2p}^x(\infty) = \frac{G_{11}}{P_{11}} = \frac{G_{44}}{P_{44}} \quad (41)$$

depending on the system and the basis set. Similar conclusions apply to the function $a_{2p}^y(t)$ with the stationary values

$$a_{2p}^y(0) = \frac{G_{22} + G_{25}}{P_{22} + P_{25}} \quad (42)$$

and

$$a_{2p}^y(\infty) = \frac{G_{22}}{P_{22}} = \frac{G_{55}}{P_{55}} \quad (43)$$

Generally, $a_{2p}^x(t) \neq a_{2p}^y(t)$, but if the system is symmetric with respect to rotation about the z axis, then $a_{2p}^x(t) = a_{2p}^y(t)$ for any direction in the xy plane intersecting the z axis at $z = t$.

In any event,

$$a_{\max} = \max\{a_{2p}^x(0), a_{2p}^x(\infty), a_{2p}^y(0), a_{2p}^y(\infty), a_{2p}^z\} \quad (44)$$

It should be noted that the formulas derived for cases 1 and 2 hold for both Gaussian- and Slater-type orbitals, whereas the formulas derived for cases 3 and 4 apply only to Gaussian orbitals. If needed, the corresponding equations for Slater-type orbitals may be derived using similar techniques.

3.3. Requirements for the basis sets

Not every finite basis set is suitable for evaluating the IE by the asymptotic-limit method. In ref 38 we showed that subtle changes in the composition of a Gaussian basis set, particularly in the choice of the most diffuse functions, can have dramatic effects on the shape and asymptotic limit of the ALEE at large r . In order for I_{ALEE} to be close to the correct IE, the most diffuse functions of the basis set must contribute to the HOMO, and this contribution must be greater than that to any lower-energy orbital. Basis sets that violate these requirements give unphysically low a_{max} values and hence IEs that are much too high.³⁸

A basis set that is unsuitable for evaluating the IE by the asymptotic limit method can often be made suitable by adding diffuse functions of proper shape at suitable locations. For instance, in the HF/6-31G* description of H₂O, the most diffuse functions (two s -type Gaussians of the H atoms) do not contribute to the HOMO (atomic p orbital of the O atom) at all, so one gets $a_{\text{max}} = -0.571 E_h$ and $\epsilon_{\text{HOMO}}^{\text{HF}} = -0.498 E_h$. By contrast, a similar HF/6-31+G* calculation on the same molecule gives $a_{\text{max}} = \epsilon_{\text{HOMO}}^{\text{HF}} = -0.509 E_h$ because the most diffuse functions of the 6-31+G* basis (p -type Gaussians of the O atom) contribute to the HOMO.

4. NUMERICAL EXAMPLES

4.1. Computational details

Extraction of the first IE from a wavefunction by the asymptotic-limit method requires computing the generalized Fock (\mathbf{G}) and density (\mathbf{P}) matrices and substituting their elements into simple relations such as eqs 29, 33, 37, and 44. We performed these calculations using a locally modified version of the GAUSSIAN program.³⁹ Matrices \mathbf{G} and \mathbf{P} were constructed from wavefunctions of three types: HF, CASSCF and FCI. The method was applied to atoms and molecules at the experimental equilibrium geometries taken from Ref. 40 and included in Table 1.

Most standard Gaussian basis sets are defined unambiguously. An important exception is Dunning’s correlation-consistent basis sets, cc-pVXZ and aug-cc-pVXZ. In the original definitions of these sets,^{41–43} the most diffuse primitive Gaussians appear both as uncontracted functions and in contractions, whereas in the transformed versions^{44,45} the most

diffuse functions appear only as uncontracted primitives. We employed the transformed variants of cc-pVXZ and aug-cc-pVXZ as implemented in the GAUSSIAN program.³⁹

To assess the accuracy of I_{ALEE} values, we compare them to the corresponding EKT IEs, denoted by I_{EKT} , and the exact values, denoted by I_{exact} , from Ref. 46 (for atoms) and the NIST Computational Chemistry Comparison and Benchmark Database⁴⁷ (for molecules other than H_2). In this work, we employ only RDMs derived from variational wavefunctions, for which the EKT gives a variational upper-bound estimate of the IE at a given level of theory. For HF wavefunctions, $I_{\text{EKT}} = -\epsilon_{\text{HOMO}}^{\text{HF}}$, which is precisely the IE implied by the rate of asymptotic decay of HF orbitals in the basis-set limit.⁴⁸⁻⁵⁰ At least within the finite-basis-set HF method, I_{ALEE} is an upper bound to I_{EKT} for reasons explained in ref 38.

4.2. Results

According to Table 1, IEs obtained by the asymptotic-limit method are in good-to-excellent agreement with the corresponding IE values obtained through the EKT, and the accuracy of both techniques generally improves with increasing level of theory. For example, the FCI/def2-QZVP wavefunction of Be gives $I_{\text{ALEE}} = 9.30$ eV and $I_{\text{EKT}} = 9.29$ eV, compared to $I_{\text{exact}} = 9.32$ eV. The ALEE and EKT CAS(8,8)/6-311+G IEs of Ne are within 0.2-0.25 eV of $I_{\text{exact}} = 21.62$ eV.

The results for the NH_3 molecule indicate that the CAS size can have a significant effect on the predicted IEs. With a suitable basis set such as DGTZVP, the full-valence CAS(8,7) wavefunction gives I_{ALEE} and I_{EKT} values that are closer to $-\epsilon_{\text{HOMO}}^{\text{HF}}$ than to I_{exact} , whereas the more accurate CAS(8,10) wavefunction gives IEs that are closer to I_{exact} than to $-\epsilon_{\text{HOMO}}^{\text{HF}}$.

Instances where I_{ALEE} is substantially higher than I_{EKT} signal a problem with the basis set. Table 1 illustrates this by examples involving LiF and H_2O . The ground-state electron configuration of LiF is $1\sigma^2 2\sigma^2 3\sigma^2 4\sigma^2 1\pi^4$, which requires the most diffuse function of the basis set to be of p type. When that is the case (cc-pVDZ, cc-pVTZ, and aug-cc-pVTZ), I_{ALEE} and I_{EKT} are in good agreement with I_{exact} and each other (within 0.3 eV). When the most diffuse function is of s type (as in aug-cc-pVTZ), it does not contribute to the HOMO and the resulting $I_{\text{ALEE}} = 15.78$ eV is much too high (by almost 4 eV).

For the H_2O molecule, the HOMO is the atomic p orbital of the O atom, so the ALEE requires a basis set whose most diffuse basis functions are p orbitals centered on the O

Table 1: First IEs (eV) extracted from correlated Gaussian-basis-set wavefunctions as the asymptotic limit of the ALEE and by using the EKT.

Method	Basis Set ^a	Case	Nucleus ^b	I_{ALEE}	I_{EKT}
		Be			
HF	def2-TZVP	1	Be	8.42	8.41
	def2-QZVP	1	Be	8.42	8.42
FCI	def2-TZVP	1	Be	9.68	9.27
	def2-QZVP	1	Be	9.30	9.29
Exact				9.32	
		Ne			
HF	6-31G	2	Ne	22.61	22.61
	6-311+G	2	Ne	23.20	23.20
CAS(8,8)	6-31G	2	Ne	20.97	20.96
	6-311+G	2	Ne	21.87	21.84
Exact				21.62	
		NH ₃ ($R_{NH} = 1.012 \text{ \AA}$, $\theta_{HNH} = 106.7^\circ$)			
HF	DGTZVP	2	N	11.66	11.64
CAS(8,7)	DGTZVP	2	N	11.58	11.55
CAS(8,10)	DGTZVP	2	N	10.60	10.57
Exact				10.82	
		LiF ($R = 1.5639 \text{ \AA}$)			
CAS(8,8)	cc-pVDZ	2	Li	11.53	11.53
	cc-pVTZ	2	Li	12.19	11.89
	aug-cc-pVDZ	2	Li	11.82	11.81
	aug-cc-pVTZ ^c	1	Li	15.78	11.96
Exact (adiabatic)				11.30	
		H ₂ O ($R_{OH} = 0.9575 \text{ \AA}$, $\theta_{HOH} = 104.51^\circ$)			
CAS(8,6)	cc-pVDZ ^c	3	H	17.10	13.49
	cc-pVTZ ^c	3	H	16.87	13.79
	aug-O-cc-pVDZ	2	O	13.92	13.92
	aug-O-cc-pVTZ	2	O	13.95	13.95
CAS(8,10)	aug-O-cc-pVDZ	2	O	12.68	12.68
	aug-O-cc-pVTZ	2	O	12.79	12.78
Exact				12.60	
		H ₂ ($R = R_e = 0.74144 \text{ \AA}$)			
FCI	cc-pVDZ	3	H	16.29	16.27
	cc-pVTZ	3	H	16.41	16.40
	cc-pVQZ	3	H	16.43	16.43
Exact				16.44	
		H ₂ ($R = 10R_e = 7.4144 \text{ \AA}$)			
FCI	cc-pVDZ	3	H	13.59	^{-d}
	cc-pVTZ	3	H	13.60	^{-d}
	cc-pVQZ	3	H	13.60	^{-d}
Exact				13.61	
		N ₂ ($R = 1.09769 \text{ \AA}$)			
CAS(10,8)	aug-cc-pVTZ	4	N	17.67	17.10
	aug-cc-pVQZ	4	N	17.66	17.10
Exact				15.58	
		F ₂ ($R = 1.41264 \text{ \AA}$)			
CAS(14,8)	aug-cc-pVTZ	4	F	18.39	17.92
	aug-cc-pVQZ	4	F	18.19	17.91
Exact				15.70	
		CH ₂ O ($R_{CO} = 1.208 \text{ \AA}$, $R_{CH} = 1.116 \text{ \AA}$, $\theta_{HCH} = 116.5^\circ$)			
CAS(12,10)	aug-O-cc-pVTZ	2	O	11.09	11.09
	aug-O-cc-pVQZ	2	O	11.10	11.10
Exact				10.88	
		C ₂ H ₄ ($R_{CC} = 1.329 \text{ \AA}$, $R_{CH} = 1.082 \text{ \AA}$, $\theta_{HCH} = 117.2^\circ$)			
CAS(12,12)	aug-C-cc-pVTZ	4	C	11.21	11.21
	aug-C-cc-pVQZ	4	C	11.21	11.21
Exact				10.68	

^aaug-A-cc-pVXZ means aug-cc-pVXZ for A, cc-pVXZ otherwise.

^bLocation of the most diffuse functions of the basis set.

^cThe most diffuse basis functions do not contribute to the HOMO.

^dThe EKT method breaks down.

nucleus. The cc-pVXZ and aug-cc-pVXZ basis sets do not satisfy this requirement (because their most diffuse functions are s orbitals of the H atom) and therefore give exaggerated I_{ALEE} values (by 3–4 eV). The problem is easily fixed by switching to the aug-cc-pVXZ basis set for the O atom while retaining cc-pVXZ for H. The composite basis sets, denoted aug-O-cc-pVXZ, give I_{ALEE} values that are in excellent agreement with I_{EKT} .

Although the EKT is more stable with respect to the type and placement of the most diffuse basis functions than the ALEE method, the latter does have one pleasing advantage. The usual manner of solving the EKT eigenvalue problem (eq 9) involves inverting the matrix $\mathbf{P}^{1/2}$. When this matrix has very small eigenvalues, it becomes ill-conditioned and the inversion breaks down.⁵¹ The asymptotic-limit method does not require inverting the \mathbf{P} matrix and therefore works even in those situations where the EKT fails. In Table 1, this is shown for a stretched H_2 molecule. Note that all instances of Case 3 in Table 1 have $a_{\text{max}} = a_{2s}^{xy}(0)$.

The remainder of Table 1 reports examples of Case 4 and illustrates applications of the asymptotic-limit method to polyatomic molecules. For CH_2O and C_2H_4 , the most diffuse basis functions should be p orbitals of the heavy atoms, a requirement that is not met by the cc-pVXZ basis sets. Using properly modified basis sets, aug-O-cc-pVXZ for CH_2O and aug-C-cc-pVXZ for C_2H_4 , we obtained $I_{\text{ALEE}} = I_{\text{EKT}}$ for these molecules. No basis-set modifications were necessary for N_2 and F_2 because the most diffuse functions of cc-pVXZ for N and F are already of proper p type. The HOMO of N_2 is a bonding orbital, whereas the HOMO of F_2 is antibonding, which is why the least negative values of $a(\mathbf{u})$ for these diatomics is found in different directions: $a_{\text{max}} = a_{2p}^x(0) = a_{2p}^y(0)$ for N_2 , but $a_{\text{max}} = a_{2p}^x(\infty) = a_{2p}^y(\infty)$ for F_2 (Fig. 2). The N_2 and F_2 molecules are the only systems in Table 1 that exhibit persistent discrepancies of about 0.5 eV between I_{ALEE} and I_{EKT} . We have not found yet a convincing explanation for this observation.

For highly stretched heteronuclear molecules such as LiH, the exact-wavefunction ALEE has a plateau around each atom at the level corresponding to the negative ionization energy of that atom.⁵² These plateaus are clearly visible⁵³ in plots of ALEEs constructed from accurate correlated wavefunctions. The true IE of such systems is the lowest IE of the constituent atoms and it could be determined by the asymptotic limit method.

Although it is not necessary to examine ALEE plots to determine a_{lim} , we note that, for most basis sets, $\bar{\epsilon}(\mathbf{r})$ visually reaches its asymptotic limits at $r = 10\text{--}20$ bohrs from the

center of the most diffuse basis function (as in Fig. 1). This distance can be much greater for Pople-style basis sets in which the exponent of the most diffuse function is shared by functions with lower l values.³⁸

5. CONCLUDING REMARKS

We have shown that the first vertical IE implied by the asymptotic behavior of the ground-state electron density can be extracted even from wavefunctions represented in terms of asymptotically incorrect Gaussian-type orbitals. The procedure is based on eq 5 and consists in finding the least negative asymptotic limit of eq 24, where \mathbf{G} and \mathbf{P} are the generalized Fock and density matrices in the atomic-orbital basis of functions $f_\mu(\mathbf{r})$. When the most diffuse functions of the basis set are Gaussian-type orbitals with $l = 0$ or $l = 1$ centered at no more than two different points, the method boils down to applying eqs 29, 33, 37, or 44.

Calculations of IEs as asymptotic limits of the ALEE do not require inverting the \mathbf{P} matrix and thus do not suffer from numerical instabilities of the EKT eigenvalue problem for systems with ill-conditioned density matrices. For such systems, the asymptotic-limit method is easier to apply and is more robust than the EKT. On the other hand, the asymptotic limit approach does not work with every Gaussian basis set and therefore cannot replace the EKT, equation-of-motion,³⁻⁵ and electron propagators¹¹ methods in general.

In order for the IE predicted by the asymptotic-limit method to be accurate, the most diffuse functions of the one-electron basis set must make nonzero contributions to the HOMO. For a given system, some standard Gaussian basis sets meet these requirements fortuitously, while others do not. When the basis set is chosen properly, IE values extracted from the ALEE are in good-to-excellent agreement with the EKT and exact IEs. Large discrepancies between I_{ALEE} and I_{EKT} indicate that the most diffuse functions of the basis set may have been chosen or assigned to atoms suboptimally. Such information may be useful as a guiding principle for developing property-optimized Gaussian basis sets for molecular response calculations.⁵⁴⁻⁵⁷

The rigorous finite-basis-set approach developed in this work can be adapted to studying the long-range behavior of other quantities and, in fact, it suggests a new way for analyzing the intricate asymptotic properties⁵⁸⁻⁶² of Kohn–Sham exchange–correlation potentials. Of

course, the long-range behavior of one-electron basis functions is not always important, and even atomic orbitals that completely vanish beyond a certain distance from the nucleus can be perfectly adequate for thermochemical predictions.⁶³

Appendix

Consider a one-electron system described with an orbital $\phi(\mathbf{r})$. By definition, $\rho(\mathbf{r}) = |\phi(\mathbf{r})|^2$, $\tau(\mathbf{r}) = \frac{1}{2}|\nabla\phi(\mathbf{r})|^2$, and $\tau_L(\mathbf{r}) = -\frac{1}{2}\phi(\mathbf{r})\nabla^2\phi(\mathbf{r})$. If $\phi(\mathbf{r})$ is a Slater-type orbital, $\phi(\mathbf{r}) = e^{-\alpha r}$, then the ratios of eq 3 and eq 4 are

$$\frac{\nabla^2\rho(\mathbf{r})}{8\rho(\mathbf{r})} = \frac{\alpha^2}{2} - \frac{\alpha}{2r} \quad (45)$$

$$\frac{\tau_W(\mathbf{r})}{\rho(\mathbf{r})} = \frac{\tau(\mathbf{r})}{\rho(\mathbf{r})} = \frac{\alpha^2}{2} \quad (46)$$

$$\frac{\tau_L(\mathbf{r})}{\rho(\mathbf{r})} = -\frac{\alpha^2}{2} + \frac{\alpha}{r} \quad (47)$$

The $r \rightarrow \infty$ limit of all these ratios is $\alpha^2/2$. On the other hand, if $\phi(\mathbf{r})$ is a Gaussian-type orbital, $\phi(\mathbf{r}) = e^{-\alpha r^2}$, then

$$\frac{\nabla^2\rho(\mathbf{r})}{8\rho(\mathbf{r})} = 2\alpha^2 r^2 - \frac{3\alpha}{2} \quad (48)$$

$$\frac{\tau_W(\mathbf{r})}{\rho(\mathbf{r})} = \frac{\tau(\mathbf{r})}{\rho(\mathbf{r})} = 2\alpha^2 r^2 \quad (49)$$

$$\frac{\tau_L(\mathbf{r})}{\rho(\mathbf{r})} = \frac{\tau(\mathbf{r})}{\rho(\mathbf{r})} - \frac{\nabla^2\rho(\mathbf{r})}{4\rho(\mathbf{r})} = 3\alpha - 2\alpha^2 r^2 \quad (50)$$

All of these ratios diverge when $r \rightarrow \infty$.

Acknowledgments

This work was supported by the Natural Sciences and Engineering Research Council (NSERC) of Canada through the Discovery Grants Program (Application RGPIN-2020-06420).

Supporting Information

Detailed specification of the cc-pVXZ and aug-cc-pVXZ basis sets used in this work, and

the SCF energies for the wavefunctions of Table 1. This information is available free of charge via the Internet at <http://pubs.acs.org>

REFERENCES

- ¹ Davidson, E. R.; Jarzęcki, A. A. Zero point corrections to vertical excitation energies. *Chem. Phys. Lett.* **1998**, *285*, 155–159.
- ² Simons, J. In *Theory and Applications of Computational Chemistry: The First Forty Years*; Dykstra, C. E., Frenking, G., Kim, K. S., Scuseria, G. E., Eds.; Elsevier: Amsterdam, 2005; pp 443–464.
- ³ Rowe, D. J. Equation-of-motion method and the extended shell model. *Rev. Mod. Phys.* **1968**, *40*, 153–166.
- ⁴ Smith, D. W.; Day, O. W. Natural transition orbitals and Rowe’s equation of motion. *Int. J. Quantum Chem. Symp.* **1974**, *8*, 511–513.
- ⁵ Szekeres, Z.; Szabados, A.; Kállay, M.; Surjan, P. R. On the “killer condition” in the equation-of-motion method: Ionization potentials from multi-reference wave functions. *Phys. Chem. Chem. Phys.* **2001**, *3*, 696–701.
- ⁶ Hunter, G. Ionization potential and conditional amplitudes. *Int. J. Quantum Chem. Symp.* **1975**, *9*, 311–315.
- ⁷ Morrell, M. M.; Parr, R. G.; Levy, M. Calculation of ionization potentials from density matrices and natural functions, and the long-range behavior of natural orbitals and electron density. *J. Chem. Phys.* **1975**, *62*, 549–554.
- ⁸ Day, Jr., O. W.; Smith, D. W. In *Reduced Density Operators with Applications to Physical and Chemical Systems-II*; Erdahl, R. M., Ed.; Queen’s University: Kingston, ON, 1974; pp 177–187.
- ⁹ Day, O. W.; Smith, D. W.; Garrod, C. A generalization of the Hartree–Fock one-particle potential. *Int. J. Quantum Chem. Symp.* **1974**, *8*, 501–509.
- ¹⁰ Smith, D. W.; Day, O. W. Extension of Koopmans’ theorem. I. Derivation. *J. Chem. Phys.* **1975**, *62*, 113–114.
- ¹¹ Ortiz, J. V. Electron propagator theory: an approach to prediction and interpretation in quantum chemistry. *WIREs Comput. Mol. Sci.* **2013**, *3*, 123–142.
- ¹² Davidson, E. R. *Reduced Density Matrices in Quantum Chemistry*; Academic: New York, 1976;

pp 55–56.

- ¹³ Ahlrichs, R. Long-range behavior of natural orbitals and electron density. *J. Chem. Phys.* **1976**, *64*, 2706–2707.
- ¹⁴ Hoffmann-Ostenhof, M.; Hoffmann-Ostenhof, T. “Schrödinger inequalities” and asymptotic behavior of the electron density of atoms and molecules. *Phys. Rev. A* **1977**, *16*, 1782–1785.
- ¹⁵ Katriel, J.; Davidson, E. R. Asymptotic behavior of atomic and molecular wave functions. *Proc. Natl. Acad. Sci. U.S.A.* **1980**, *77*, 4403–4406.
- ¹⁶ Almbladh, C.-O.; Pedroza, A. C. Density-functional exchange-correlation potentials and orbital eigenvalues for light atoms. *Phys. Rev. A* **1984**, *29*, 2322–2330.
- ¹⁷ Levy, M.; Perdew, J. P.; Sahni, V. Exact differential equation for the density and ionization energy of a many-particle system. *Phys. Rev. A* **1984**, *30*, 2745–2748.
- ¹⁸ Cuevas-Saavedra, R.; Ayers, P. W.; Staroverov, V. N. Kohn–Sham exchange-correlation potentials from second-order reduced density matrices. *J. Chem. Phys.* **2015**, *143*, 244116.
- ¹⁹ Koopmans, T. Über die Zuordnung von Wellenfunktionen und Eigenwerten zu den einzelnen Elektronen eines Atoms. *Physica* **1934**, *1*, 104–113.
- ²⁰ Morrison, R. C.; Liu, G. Extended Koopmans’ theorem: Approximate ionization energies from MCSCF wave functions. *J. Comput. Chem.* **1992**, *13*, 1004–1010.
- ²¹ Cioslowski, J.; Piskorz, P.; Liu, G. Ionization potentials and electron affinities from the extended Koopmans’ theorem applied to energy-derivative density matrices: The EKTMP n and EKTQCISD methods. *J. Chem. Phys.* **1997**, *107*, 6804–6811.
- ²² Bozkaya, U. The extended Koopmans’ theorem for orbital-optimized methods: Accurate computation of ionization potentials. *J. Chem. Phys.* **2013**, *139*, 154105.
- ²³ Gu, Y.; Xu, X. Extended Koopmans’ theorem at the second-order perturbation theory. *J. Comput. Chem.* **2020**, *41*, 1165–1174.
- ²⁴ Ryabinkin, I. G.; Staroverov, V. N. Average local ionization energy generalized to correlated wavefunctions. *J. Chem. Phys.* **2014**, *141*, 084107.
- ²⁵ Hinze, J. MC-SCF. I. The multi-configuration self-consistent-field method. *J. Chem. Phys.* **1973**, *59*, 6424–6432.
- ²⁶ Siegbahn, P. E. M.; Almlöf, J.; Heiberg, A.; Roos, B. O. The complete active space SCF (CASSCF) method in a Newton–Raphson formulation with application to the HNO molecule. *J. Chem. Phys.* **1981**, *74*, 2384–2396.

- ²⁷ Helgaker, T.; Jørgensen, P.; Olsen, J. *Molecular Electronic-Structure Theory*; Wiley: Chichester, 2000.
- ²⁸ Löwdin, P.-O. Quantum theory of many-particle systems. I. Physical interpretations by means of density matrices, natural spin-orbitals, and convergence problems in the method of configurational interaction. *Phys. Rev.* **1955**, *97*, 1474–1489.
- ²⁹ Smith, V. H.; Öhrn, Y. In *Reduced Density Operators with Applications to Physical and Chemical Systems-II*; Erdahl, R. M., Ed.; Queen’s University: Kingston, ON, 1974; pp 193–200.
- ³⁰ McWeeny, R. *Methods of Molecular Quantum Mechanics*, 2nd ed.; Academic Press: London, 1989; pp 261–262.
- ³¹ Pernal, K.; Cioslowski, J. Ionization potentials from the extended Koopmans’ theorem applied to density matrix functional theory. *Chem. Phys. Lett.* **2005**, *412*, 71–75.
- ³² Cuevas-Saavedra, R.; Staroverov, V. N. Exact expressions for the Kohn–Sham exchange–correlation potential in terms of wave-function-based quantities. *Mol. Phys.* **2016**, *114*, 1050–1058.
- ³³ Staroverov, V. N. Contracted Schrödinger equation and Kohn–Sham effective potentials. *Mol. Phys.* **2019**, *117*, 1–5.
- ³⁴ Kohut, S. V.; Cuevas-Saavedra, R.; Staroverov, V. N. Generalized average local ionization energy and its representations in terms of Dyson and energy orbitals. *J. Chem. Phys.* **2016**, *145*, 074113.
- ³⁵ Ryabinkin, I. G.; Kohut, S. V.; Cuevas-Saavedra, R.; Ayers, P. W.; Staroverov, V. N. Response to “Comment on ‘Kohn–Sham exchange–correlation potentials from second-order reduced density matrices’” [J. Chem. Phys. **145**, 037101 (2016)]. *J. Chem. Phys.* **2016**, *145*, 037102.
- ³⁶ Mura, M. E.; Knowles, P. J.; Reynolds, C. A. Accurate numerical determination of Kohn–Sham potentials from electronic densities: I. Two-electron systems. *J. Chem. Phys.* **1997**, *106*, 9659–9667.
- ³⁷ Schipper, P. R. T.; Gritsenko, O. V.; Baerends, E. J. Kohn–Sham potentials corresponding to Slater and Gaussian basis set densities. *Theor. Chem. Acc.* **1997**, *98*, 16–24.
- ³⁸ El-Samman, A. M.; Staroverov, V. N. Asymptotic behavior of the average local ionization energy in finite basis sets. *J. Chem. Phys.* **2020**, *153*, xxxxxx. DOI: 10.1063/5.0023459
- ³⁹ Frisch, M. J.; Trucks, G. W.; Schlegel, H. B.; Scuseria, G. E.; Robb, M. A.; Cheeseman, J. R.; Scalmani, G.; Barone, V.; Petersson, G. A.; Nakatsuji, H.; et al. *Gaussian Development Version*,

- Revision I.13*; Gaussian, Inc.: Wallingford, CT, 2016.
- ⁴⁰ Rumble, J. R., Ed. *CRC Handbook of Chemistry and Physics*, 99th ed.; CRC Press: Boca Raton, FL, 2018.
- ⁴¹ Dunning, Jr., T. H. Gaussian basis sets for use in correlated molecular calculations. I. The atoms boron through neon and hydrogen. *J. Chem. Phys.* **1989**, *90*, 1007–1023.
- ⁴² Kendall, R. A.; Dunning Jr., T. H.; Harrison, R. J. Electron affinities of the first-row atoms revisited. Systematic basis sets and wave functions. *J. Chem. Phys.* **1992**, *96*, 6796–6806.
- ⁴³ Pritchard, B. P.; Altarawy, D.; Didier, B.; Gibson, T. D.; Windus, T. L. A new Basis Set Exchange: An open, up-to-date resource for the molecular sciences community. *J. Chem. Inf. Model.* **2019**, *59*, 4814–4820.
- ⁴⁴ Hashimoto, T.; Hirao, K.; Tatewaki, H. Comment on Dunning’s correlation-consistent basis sets. *Chem. Phys. Lett.* **1995**, *243*, 190–192.
- ⁴⁵ Davidson, E. R. Comment on “Comment on Dunning’s correlation-consistent basis sets”. *Chem. Phys. Lett.* **1996**, *260*, 514–518.
- ⁴⁶ Chakravorty, S. J.; Gwaltney, S. R.; Davidson, E. R.; Parpia, F. A.; Froese Fischer, C. Ground-state correlation energies for atomic ions with 3 to 18 electrons. *Phys. Rev. A* **1993**, *47*, 3649–3670.
- ⁴⁷ Johnson III, R. D., Ed. *NIST Computational Chemistry Comparison and Benchmark Database*, NIST Standard Reference Database Number 101, Release 29 (August 2019), <http://cccbdb.nist.gov> (accessed on July 31, 2020), DOI: 10.18434/T47C7Z.
- ⁴⁸ Handy, N. C.; Marron, M. T.; Silverstone, H. J. Long-range behavior of Hartree–Fock orbitals. *Phys. Rev.* **1969**, *180*, 45–48.
- ⁴⁹ Handler, G. S.; Smith, D. W.; Silverstone, H. J. Asymptotic behavior of atomic Hartree–Fock orbitals. *J. Chem. Phys.* **1980**, *73*, 3936–3938.
- ⁵⁰ Ishida, T.; Ohno, K. On the asymptotic behavior of Hartree–Fock orbitals. *Theor. Chim. Acta* **1992**, *81*, 355–364.
- ⁵¹ Morrison, R. C.; Dixon, C. M.; Mizell Jr., J. R. Examination of the limits of accuracy of the extended Koopmans’ theorem ionization potentials into excited states of ions of LiH, He₂, and Li₂. *Int. J. Quantum Chem. Symp.* **1994**, *28*, 309–314.
- ⁵² Gritsenko, O. V.; Baerends, E. J. Effect of molecular dissociation on the exchange–correlation Kohn–Sham potential. *Phys. Rev. A* **1996**, *54*, 1957–1972.

- ⁵³ Kohut, S. V.; Polgar, A. M.; Staroverov, V. N. Origin of the step structure of molecular exchange-correlation potentials. *Phys. Chem. Chem. Phys.* **2016**, *18*, 20938–20944.
- ⁵⁴ Rappoport, D.; Furche, F. Property-optimized Gaussian basis sets for molecular response calculations. *J. Chem. Phys.* **2010**, *133*, 134105.
- ⁵⁵ Rappoport, D. Basis-set quality and basis-set bias in molecular property calculations. *ChemPhysChem* **2011**, *12*, 3404–3413.
- ⁵⁶ Jensen, F. Atomic orbital basis sets. *WIREs Comput. Mol. Sci.* **2013**, *3*, 273–295.
- ⁵⁷ Nagy, B.; Jensen, F. Basis sets in quantum chemistry. *Rev. Comput. Chem.* **2017**, *30*, 93–149.
- ⁵⁸ Della Sala, F.; Görling, A. Asymptotic behavior of the Kohn–Sham exchange potential. *Phys. Rev. Lett.* **2002**, *89*, 033003.
- ⁵⁹ Kümmel, S.; Perdew, J. P. Simple iterative construction of the optimized effective potential for orbital functionals, including exact exchange. *Phys. Rev. Lett.* **2003**, *90*, 043004.
- ⁶⁰ Wu, Q.; Ayers, P. W.; Yang, W. Density-functional theory calculations with correct long-range potentials. *J. Chem. Phys.* **2003**, *119*, 2978.
- ⁶¹ Gori-Giorgi, P.; Gál, T.; Baerends, E. J. Asymptotic behaviour of the electron density and the Kohn–Sham potential in case of a Kohn–Sham HOMO nodal plane. *Mol. Phys.* **2016**, *114*, 1086–1097.
- ⁶² Gori-Giorgi, P.; Baerends, E. J. Asymptotic nodal planes in the electron density and the potential in the effective equation for the square root of the density. *Eur. Phys. J. B* **2018**, *91*, 160.
- ⁶³ McKemmish, L. K.; Gilbert, A. T. B.; Gill, P. M. W. Mixed ramp-Gaussian basis sets. *J. Chem. Theory Comput.* **2014**, *10*, 4369–4376.